RSC Advances

ROYAL SOCIETY OF CHEMISTRY

www.rsc.org/advances

Polymethylmethacrylate doped with porphyrin and silver nanoparticles as light-activated antimicrobial material

O. Lyutakov[a,*], O. Hejna[a], A. Solovyev[b], Y. Kalachyova[a] and V. Svorcik[a]

[a] *Department of Solid State Engineering, Institute of Chemical Technology, Prague 166 28, Czech Republic, [*]E mail : lyutakoo@vscht.cz*

[b] *Institute of Chemical Process Fundamentals of the AS CR, Prague 165 02, Czech Republic*

Abstract

Light-activated antimicrobial materials on the base of polymethylmethactylate doped with porphyrin and silver nanoparticles was prepared and studied. The inspiration for the material design originates from photodynamic therapy where light is used to destroy pathogen microbes. Antimicrobial response of the materials is controlled by blue light illumination. Porphyrin molecules serve as light absorber with dual antimicrobial response - under illumination they produce reactive oxygen and affect kinetics of silver release from polymer. Silver is responsive for antimicrobial effect, for protection of porphyrin against photobleaching and for conservation of energy through suppression of porphyrin luminescence. Triggerable and enhanced antimicrobial response of the material is activated thought several possible mechanisms, including local heating of polymer matrix, transfer of excited state from porphyrin to silver and synergetic effect of reactive oxygen and silver. In a passive state the material exhibits weak antimicrobial response against gramm-negative bacteria. In an active state, however, it is fatal for both, gramm negative and gramm positive bacteria.

1 Introduction

The rising problem of antibiotic resistance has led to fears that medicine will return to "before-penicillin era" when significant mortality of patients occurred due to uncontrollable infection. Application of new, more effective classes of antibiotics cannot solve the problem "in principum" and only postpone medicine collapse. Pathogenic bacterial strains harboring drug resistance genes are frequently found in hospitals and clinics.[1] These bacteria may not cause serious health complications outside a clinical environment, but in a healthcare setting it may result in morbidity of debilitated patients. Thus, alternative strategies and approach for antimicrobial treatment of resistant bacteria are extremely needed. Among the new strategies there are two prominent approach, which rely on antibiotics substitution by metal nanoparticles (MeNPs) or antimicrobial peptides and on the application of light treatment.[2] Silver NPs exhibit most pronounced antimicrobial effect among metal NPs. AgNPs destroy bacteria walls and thus disrupt intracellular balance.[3] Additionally, AgNPs can be combined with antibiotics, where AgNPs perforate cell membrane and allow antibiotics to penetrate inside. Significant decreasing of bacteria level was reported for simultaneous treatment of bacteria by sub-lethal concentration of AgNPs and antibiotics.[4] Efficiency of AgNPs can vary with different kinds of bacteria and furthermore can be different from one stamp to another. In general, AgNPs are more effective against gramm-negative bacteria, than gramm-positive ones.[3] Toxicity effect of silver compounds can be reduced by their combination with polymeric nanocarriers.[5]

Another alternative approach is light-based photo dynamic therapy (PDT). This therapy can eradicate microbes regardless of antibiotic resistance.[6] Mechanism of light treatment lies in the production of reactive oxygen (RO) by chromophores under illumination. RO chemically attacks a very wide range of biomolecules and where one microorganism is naturally resistant to RO species attack at one site, it may be impressible to another site. Therefore the bacteria kill is still successful reducing the evolution of resistance against light treatment.[7,8] Despite the numerous attempts to induce resistance by repeated cycles of sublethal PDT and microbial re-growth there have been no reported cases of PDT induced resistance of microorganisms.[9,10] Moreover, PDT demonstrated significant killing effects on some bacteria which are very difficult to inactivate by antibiotics.[11]

Light can be used for direct antimicrobial treatment or for RO production by artificially added photosensitisers (PS). Direct light treatment affects the intracellular chromophores and can selectively kill bacteria, depending on the applied wavelength (usually UV) and exposure dose. However, one must consider the possible side effects of UV irradiation, delivered at effective antimicrobial fluencies on normal mammalian cells and tissue. At the other hand photo dynamic therapy (PDT) utilizes artificially introduced PS which can produce RO under visible light

illumination and thus allows antimicrobial treatment with more lenient wavelength. It was found, that PS concentrations and illumination dose that effectively reduced bacterial levels, did not damage mammalian cells.[9]

Porphyrin and related compounds are commonly used in PDT because they can effectively produce RO upon visible light irradiation.[12,13] Clinical applications of porphyrin-based PDT includes dental disease, cutaneous superficial and subcutaneous infection, gastric infections, and so on therapies.[14] However, porphyrin can undergo photobleaching under illumination, and this sufficiently restricts its long-term practical utilization. Presence of additional antimicrobial agents may improve porphyrin stability and enhance its effectiveness. In the work[15] chemical stability of the porphyrin was enhanced by its introduction into Zn_2Al LDH matrix. Synergetic effect of porphyrin encapsulated into ZnO was described too.[9] Similarly, AuNPs and PS doped polymer was also successfully applied for preventing of biofilm formation.[16] Studies showed that PS in combination with size-specific gold nanoparticles demonstrates enhanced light-activated antimicrobial activity, compared to PS only.[17,18]

Antimicrobial efficacy of PDT can be further exploited through the fixation of these molecules in support materials and resultant materials appear to be effectively self-sterilizing.[19] Different material supports have thus been proposed, including cellulose, silica, textiles, and glass, the PS may be entrapped or absorbed, or covalently attached to the surface of the carrier.[20,21] Porphyrin based photobactericidal materials have been developed by grafting porphyrin-based compounds onto nylon fibers,[13] alkylated cellulose[22] and poly(methylmetchacrylate) (PMMA).[19,23]

In this work we report about light-activated antimicrobial material based on PMMA doped with physically interacting porphyrin and silver nanoparticles. Antimicrobial response of the proposed materials is controlled by blue light illumination. Porphyrin molecules serve as light absorber with dual antimicrobial response. Silver is responsible for antimicrobial effect, for protection of porphyrin against photobleaching and for conservation of energy through suppression of porphyrin luminescence. Triggerable and enhanced antimicrobial response (gramm negative and gramm positive) bacteria is activated thought several possible mechanisms, including local heating of polymer matrix, transfer of excited state from porphyrin to silver and synergetic effect of reactive oxygen and silver. We estimated coupling of AgNPs and porphyrin by absorption and luminescence spectroscopies. Dynamic of silver release was determined using atomic absorption and x-ray photo spectroscopies. Finally light switchable antimicrobial properties were examined on *P.aeruginosa* and *S.aureus* bacteria strains.

2 Experimental aspects

2.1 Materials

Anhydrous N-methyl-2-pyrrolidone (NMP, 99.5 %, Sigma Aldrich) and silver nitrate (99.9999 %, Sigma Aldrich), were used as received. Polymethylmethacrylate (PMMA, M_w=1459000, Goodfellow) of "optical" purity was also used as received. Tetraphenylporphine (TPP), 99 % purity, was supplied from Frontier Scientific. Mueller-Hinton broth (MHB) (Oxoid, CM0405) and Mueller-Hinton agar (MHA) (Oxoid, CM0337) were prepared as described by producer and sterilized by autoclave.

2.2 Sample preparation

The samples were distributed to three test groups:

(i) Only porphyrin (TPP/PMMA) – 0.015 g TPP was dissolved in 5 g of n-methylpyrrolidone and mixed with 7 % solution of PMMA in dichlorethane. Then obtained solution was spin-coated at 1000 rpm for 15 s onto hot plate (200^o C) up to solvent evaporation. Concentration of TPP in the dried polymer film was 5 %.

(ii) Only AgNPs (AgNPs/PMMA) – silver nitrate (0.095 g) was dissolved in 5 g of n-methylpyrrolidone and mixed with 7 % solution of PMMA in dichlorethane. Then obtained solution was spin-coated at 1000 rpm for 15 s onto hot plate (200°C) up to appearance of uniform yellow coloring. Creation of AgNPs under these conditions was described in our previous works.[24] Concentration of silver in the dried polymer film was 10 %.

(iii) AgNPs and porphyrin (TPP-AgNPs/PMMA) – silver nitrate and TPP (0.03 g and 0.095 g) were dissolved in n-methylpyrrolidone and mixed with 7 % solution of PMMA in dichlorethane. Then obtained solution was spin-coated at 1000 rpm for 15 s and rapidly placed at hot plate (200°C) up to solvent evaporation and appearance of uniform coloring. Concentrations of Ag and TPP in the dried polymer film were 10 and 5 % respectively.

2.3 Sample treatment and characterization

Polymer films thicknesses were measured by profilometry technique (Hommel Tester T 1000 profilometer, scratch method) and found to be 3 μm in all cases. Sample treatment was performed by soaking in distilled water, irradiation with blue light, and combination of light and water treatments. As a light source Light-Emitting Diode (LED) with 110 mW power output and 405 nm center wavelength was used. The light was focused into circular spot with diameter 1.2 cm.

UV-Vis spectra were measured using Spectrometer Lambda 25 (Perkin-Elmer) in 330-600 nm wavelength range. Photoluminescence spectra (excitation wavelengths 417 and 424 nm) were obtained by using fluorescent spectrophotometer SPECTRA star Omega. Creation and distribution of AgNPs were determined by transmission electron microscopy (TEM) on JEOL JEM-1010 instrument operated at 80 kV. Recovery of silver to Ag^0 by oxidation was described in our previous work[24]. The same work describes the conversion rate of silver under the given experimental conditions, which is 78 %. Concentration of released silver was determined by atomic absorption spectroscopy (AAS) on Varian AA 880 device. Residual amount of silver was estimated from X-ray induced photoelectron spectra (XPS) measured on Omicron Nanotechnology ESCAProbeP spectrometer. Electron beam etching was additionally applied between subsequent XPS measurements to measure Ag depth profile. Production of reactive oxygen was proved using iodometry followed by absorption spectroscopy measurements.

2.4 Antimicrobial tests

The antibacterial effect of all samples on two environmental bacterial strains: (i) gramm-negative *Pseudomonas aeruginosa* (*P.aeruginosa*) and (ii) gramm-positive *Staphylococcus aureus* (*S.aureus*) was studied. Two sets of experiments were performed – study of antimicrobial activity in solution and in contact. *In solution* - all types of samples were inoculated together with the diluted solutions of *S.aureus* or *P.aeruginosa* (concentration 10^3 cells ml^{-1}). Solution without added samples served as a dark control. Inoculated solutions were incubated at laboratory temperature in static conditions for 0.5, 6 and 24 h simultaneously irradiation with LED was performed. The LED was placed at a distance of 15 cm above the sample. Dark incubated samples, containing only AgNPs (with and without illumination) and only TPP (with and without illumination) and irradiated bacteria suspension without samples (light control) were used as control ones in each experiment. Aliquots of treated suspension were singled after different time intervals and placed on LB agar plates. The growth of *S.aureus* and *P.aeruginosa* was evaluated after 24 h. Each sample was evaluated separately in triplicate. *In contact* - alternatively, the samples were attached onto agar plates previously colonized by bacteria (1 ml of bacteria suspension containing $5x10^7$ bacteria cells in both cases) and irradiated for different times. The LED was placed at a distance of 15 cm above the sample. As a control non-irradiated samples and irradiated pristine PMMA were used. After irradiation the agar plates were placed in incubator and bacteria growth was evaluated after 24 h.

3 Results and discussion

In principle, PDT has been shown to be more effective against Gram-positive than Gram-negative bacteria.[25,26] At the other hand, AgNPs antimicrobial effect is more pronounced in the case of gramm-negative bacteria.[3,27,28] In this paper we combine PDT and AgNPs antimicrobial properties for treating of both Gram-positive and Gram-negative bacteria. We also expect additional antimicrobial effect arising from the interaction of AgNPs and PS.

Creation of AgNPs was confirmed by TEM method. Fig. 1 shows AgNPs allocation in polymer film. Prepared AgNPs have size distribution in 5-25 nm range. In many cases AgNPs with non-spherical shapes were observed. In the Fig. 1 triangular and polygonal nanoparticles are marked by blue arrows. Creation of AgNPs with angular shapes by n-methylpyrrolidone or polyvinylpyrrolidone reduction have also been frequently observed.[29,30] It should be noted, that sharp NPs edges act as “hot places”, where the light intensity is especially high.

Thus, angular shape of AgNPs is expected to enhance plasmon-related optical properties of nanoparticles. Fig. 2 depicts optical absorption and luminescence properties of TPP in the presence or absence of AgNPs. Absorption peak at 417 nm of pristine TPP (Fig. 2, left) is typical for porphyrine Soret band. It arises from delocalized π-electrons in porphyrin macrocycle. Proximity of metal nanoparticles to porphyrine can affect π-electrons and initiate shift of the Soret band. Observed “red shift” of TPP Soret band (Fig. 2, left) in the presence of AgNPs indicates the physical coupling of TPP and AgNPs.[31] Optical luminescence of TPP is also well known phenomenon.[32] Fig. 2 (right) shows luminescence of TPP/PMMA and TPP-AgNPs/PMMA films. Luminescence excitation wavelengths were selected to correlate with maxima of absorbance peaks (417 and 424 nm). From Fig. 2 (right) it is evident that optical luminescence is completely suppressed by the presence of AgNPs. Luminescence suppression occurs due to transfer of TPP excited state on AgNPs and this also confirms TPP and NPs mutual coupling. Quite complete suppression confirms the high efficiency of the energy transfer. This phenomenon conserves energy in the system, which would otherwise been lost in the form of secondary radiation, and allows inference of AgNPs on TPP and vice versa – TPP on AgNPs.

Effect of porphyrin illumination on the kinetic of silver release from TPP-AgNPs/PMMA films is shown in the Fig. 3. Fig. 3A shows the cumulative release of silver from the TPP-AgNPs/PMMA films with and without illumination. Surface morphologies of AgNPs doped PMMA films before and after silver releasing were studied and reported in our previous work.[24] From Fig. 3A it is evident, that at early stages the illumination speeds silver releasing. At the same time this effect completely disappears in the later illumination stages. It is apparent, that at early stages AgNPs situated close to surface are released predominantly. Thus it can be concluded, that

the light illumination speeds AgNPs release from near surface region and slightly slows down release from deeper regions. Residual amount of silver was estimated using XPS method combined with plasma etching too. Depth profiles of silver concentration are shown in Fig. 3B for pristine, illuminated and non illuminated samples. It is evident, that after the sample preparation silver distribution is non-uniform – the concentration being sufficiently higher near the surface. This can be explained by AgNPs expulsion during the sample preparation. Samples soaking lead to decrease of silver concentration predominantly in near surface region. The effect is more pronounced, when the sample is simultaneously irradiated. In general, results of XPS confirm AAS studies, i.e. the excitation of TPP in TPP-AgNPs/PMMA films enhances AgNPs release form the sample surface.

Results of samples soaking in water (H_2O), long-term illumination (*hv*) and in water under illumination (H_2O/*hv*) were obtained by UV-Vis absorption spectroscopy (see Fig. 4). The wavelength range was the same for all figures. Absorbance values for all figures are given on the left hand side. From Fig. 4 it is evident, that TPP (TPP/PMMA film) exhibits tendency to degrade under illumination and this leads to a decrease of Soret band signal. Concentration of AgNPs (AgNPs/PMMA film) under sample soaking slightly decreases as can be seen from a decrease of NPs related plasmon absorption band. This effect may be due to AgNPs release from PMMA matrix. Illumination of AgNPs/PMMA film, however, increases plasmon band amplitude, probably due to silver reduction and creation of additional AgNPs. When the AgNPs/PMMA was simultaneously soaked and illuminated a decrease of the plasmon absorption band is observed, indicating that the leaching of silver becomes dominant process. In the case of TPP-AgNPs/PMMA film AgNPs plasmon absorption band is masked by intensive Soret band and it is not visible. When TPP-AgNPs/PMMA samples were illuminated by light only slight decrease of Soret band was observed. This indicates that TPP was effectively protected by AgNPs. To verify this result we irradiate the TPP-AgNPs/PMMA in water repeatedly three times (bottom, right part of Fig. 4 – 72h of sample treatment) but a further decrease of Soret band was not observed. This observation indicates that the TPP structure is well protected against photobleaching by coupling with AgNPs. It must be noted, that both Soret band intensity and position are conserved under illumination of TPP-AgNPs/PMMA samples. Conservation of Soret band intensity indicates preservation of TPP macrocycle. On the other hand conservation of Soret band position indicates preservation of side-chain substituents in the macrocycle.

The effect of AgNPs on RO production in TPP was also examined and the ability of RO to induce iod (I^-) reduction was chosen as an indicator. Production of I_2 manifests itself by yellow coloring of initially opaque potassium iodide KI solution (appearance of pronounced absorption band at 330 nm). Possibility of I^- reduction by light illumination was also taken into account. Fig. 5

presents absorption spectra of KI solution illuminated in the presence of pristine PMMA (iodine reduction by light), TPP/PMMA (iodine reduction by RO and light), and TPP-AgNPs/PMMA films. Fresh samples and samples previously treated by light illumination in water during 72 h. were tested. Absorption peak below 400 nm is attributed to I_2. From Fig. 5 it is evident, that light irradiation causes iodine reduction. However, when TPP/PMMA and TPP-AgNPs/PMMA samples are irradiated iodine reduction is more apparent. These differences are attributed to RO production by TPP. It is also evident, that TPP/PMMA produce RO more efficiently. In the next pretreated TPP/PMMA and TPP-AgNPs/PMMA were irradiated to estimate long-term stability of RO creation. Subsequently, irradiation of films in KI solution was repeated. Results are also presented in Fig. 5. It is evident, that TPP/PMMA completely lost the ability to produce RO. At the other hand, the creation of RO by TPP-AgNPs/PMMA does not change significantly comparing to untreated samples. It can be therefore concluded, that AgNPs affect the RO production adversely, but this effect is completely compensated by higher stability of TPP in the presence of AgNPs.

In next experiments the antimicrobial properties of AgNPs/PMMA, TPP/PMMA, and TPP-AgNPs/PMMA were investigated. We tested these coatings on two bacterial strains to compare efficiency against gramm-positive and gramm-negative bacteria. Studies were performed in solution. Then the effect of light activation of TPP-AgNPs/PMMA was studied. These tests were performed in contact, by sample attached onto previously colonized agar plate. In each case control experiments on bacteria growth affected by only pristine PMMA or light irradiation were accomplished.

In dark control experiments no bacteria growth inhibition was observed. In light control experiments only weak reduction of bacteria growth was observed, probably due to RO production by intracellular chromophores. Table 1 gives the antimicrobial efficiencies of AgNPs/PMMA, TPP/PMMA, and TPP-AgNPs/PMMA samples on *P.aeruginosa* and *S.aureus* with/and without illumination. Negative sign means absence of antimicrobial effect (see Fig. 6), positive sign indicates the case of fully destroyed bacteria, plus/minus sign corresponds to an intermediate case. AgNPs/PMMA samples were effective in the case of gramm-negative bacteria. Illumination slightly reduced their antimicrobial effect. In the case of *S.aureus* AgNPs only very weak antimicrobial effect is found. At the other hand TPP/PMMA films were more effective against *S.aureus*. For activation of their antimicrobial properties illumination was necessary. TPP/PMMA films showed only weak effect against *P.aeruginosa* of bacteria. In general, the Gram-positive bacteria were inactivated faster than Gram-negative ones in the case of TPP.[31] At the other hand AgNPs are highly active against gramm-negative bacteria.[24] As to TPP-AgNPs/PMMA films, they were effective against both, gramm-negative and gramm-positive bacteria, but mainly in “active”,

illuminated state. Only weak activity against gramm-negative bacteria of TPP-AgNPs/PMMA in dark was observed which may be attributed to spontaneous diffusion of silver. For sufficient activation of TPP-AgNPs/PMMA antimicrobial properties the illumination is needed. We also perform test of $AgNO_3$ solution in distilled water with $5x10^{-6}$ g ml^{-1} Ag^+ concentration. This concentration is the same order as the silver amount which can be released from fully leached films. Results are also given in the Tab. 1. It is evident, that $AgNO_3$ solution acts effectively on gram-negative and less effective on gram positive bacteria.

Light-switchable properties of TPP-AgNPs/PMMA films were examined. These experiments were performed in ”contact” mode, i.e. samples were placed in contact with previously cultivated on agar bacteria. The irradiation with light-emitting diode for 0.5, 1, and 3 hours was applied. Non-illuminated sample (3 hours) was chosen as a control one. Results are presented in Fig. 7. Lighter areas in the figure (similar in color to surrounding agar) correspond to the development of many bacterial microcolonies and to the absence of antimicrobial properties. Lighter areas were observed in both controls and samples irradiated during 0.5 h. The bright points on the figure correspond to the development of individual colonies. In this case, the antimicrobial properties are fully manifested, but some bacteria still survived. This same situation was observed in the case of samples irradiated during 2 h. Irradiation during 3 h led to the complete destruction of *S.aureus*, but only to partial destruction of *P.aeruginosa*. In general, antimicrobial properties were fully controlled by light switch-on/off. In the case of continuous illumination the major bacteria reduction was observed after 90-180 min. Finally, additional parts “E” in Fig. 7 shows antimicrobial properties of samples stored for three months at ambient conditions (sunlight, normal air). Both samples were light-activated during 3 h. It is evident that antimicrobial activity of the aged samples slightly decreased in the case of *P.aeruginosa* and remained completely unchanged in the case of *S.aureus.*

4 Conclusion

Functional coatings become a key component in the striving to keep healthcare environments microbe free. Light activated antimicrobial materials could be deployed in many forms including protective layers on medical devices or problematic places in hospitals. However, the potential use of common photoactive bactericidal materials is restricted to the class of Gram-positive bacteria.

In this paper we describe the design, preparation and properties of light-activated antimicrobial coatings based on polymethylmethactylate doped with physically interacted porphyrin and silver nanoparticles, which are effective against both, Gramm-positive and Gramm-negative bacteria. Activity of coatings was switched through blue light illumination so when the light is

switched on the microbial killing is done. Antimicrobial properties were realized through light-controllable silver release and production of active oxygen. Active oxygen was produced by porphyrine in the presence of silver nanoparticles. Interaction with AgNPs increases porphyrine stability and affects positively the kinetics of silver release. Apparently, silver was responsible for antimicrobial effect against Gram-negative bacteria and reactive oxygen killed Gram-positive bacteria. Additionally the combination of PDT with AgNPs increases the efficiency of bacterial inactivation. Proposed novel antimicrobial material in combination with a simple light system can be utilized in the development of a range of photobactericidal polymeric medical devices and coatings.

Acknowledgements

This work was supported by GACR under project P108/12/G108.

References

1 S. G. Bell, *Neonatal. Netw.,* 2003, **22**, 47-54.

2 H. L. Karlssona, P. Cronholm, Y. Hedberg, M. Tornberg, L. De Batticee, S, Svedheme and I. Odnevall Wallinder, *Toxicology,* 2013, **313**, 59-69.

3 J. S. Kim, E. Kuk, K. N. Yu, J. H. Kim, S. J. Park, H. J. Lee, S. H. Kim, Y. K. Park, C. Y. Hwang, Y. K. Kim, Y. S. Lee, D. H. Jeong and M. H. Cho, *Nanomed.-Nanotechnol. Biol. Med.,* 2007, **3**, 95-101.

4 A. R. Shahverdi, A. Fakhimi, H. R. Shahverdi and S. Minaian, *Nanomed.-Nanotechnol. Biol. Med.,* 2007, **3**, 168-171.

5 P. N. Shah, L. Y. Lin, J. A. Smolen, J. A. Tagaev, S. P. Gunsten, D. S. Han, G. S. Heo, Y. Li, F. Zhang, S. Zhang, B. D. Wright, M. J. Panzner, W. J. Youngs, S. L. Brody, K. L. Wooley, and C. L. Cannon, *ACS Nano,* 2013, **7**, 4977-4987.

6 R. Yin, T. Dai1, P. Avci, A. E. S. Jorge, W. de Melo, D. Vecchio, Y.-Y. Huang, A. Gupta and M. R. Hamblin, *Curr. Opin. Pharmacol.,* 2013, **13**, 731-762.

7 D. Mitton and R. A. Ackroyd, *Photodiagnosis Photodyn. Ther.,* 2008, **5**, 103-111.

8 T. Maisch, C. Bosl, R. M. Szeimies, N. Lehn and C. Abels, *Antimicrob. Agents Chemother.,* 2005, **49**, 1542-1552.

9 S. Senthilkumar, R. Hariharan, A. Suganthi, M. Ashokkumar, M. Rajarajan and K. Pitchumani, *Powder Technol.,* 2013**, 237**, 497-505.

10 M. Wainwright, *Photodiagnosis Photodyn. Ther.,* 2009, **6**, 167-169.

11 Y. Su, J. Sun, S. Rao, Y. Cai and Y. Yang, *J. Photochem. Photobiol. B,* 2011, **103**, 29-34.

12 F. Javed, L. P. Samaranayake and G. E. Romanos, *Photochem. Photobiol. Sci.,* 2014, **13**, 726-734.

13 J. Bozja, J. Sherrill, S. Michielsen and I. Stojiljkovic, *J. Polym. Sci. Polym. Chem.,* 2003, **41**, 2297-2303.

14 Y. Qin, X. Luan, L. Bi, G. He, X. Bai, C. Zhou and Z. Zhang, *Lasers Med. Sci.,* 2008, **23**, 49-54.

15 M. Merchan, T. S. Ouk, P. Kubat, K. Lang, C. Coelho, V. Verney, S. Commereuc, F. Leroux, V. Sol and C. Taviot-Gueho, *J. Mater. Chem. B,* 2013, **1**, 2139-2146.

16 S. Perni, P. Prokopovich, I. P. Parkin, M. Wilson and J. Pratten, *J. Mater. Chem.,* 2010, **20**, 8668-8673.

17 A. J. T. Naik, S. Ismail, C. Kay, M. Wilson and I. P. Parkin, *Mater. Chem. Phys.,* 2011, **129**, 446-450.

18 S. Perni, C. Piccirillo, J. Pratten, P. Prokopovich, W. Chrzanowski, I. P. Parkin and M. Wilson, *Biomaterials,* 2009, **30**, 89-93.

19 A. Almeida, A. Cunha, N. C. Gomes, E. Alves, L. Costa and M. A. Faustino, *Mar. Drugs,* 2009, **7**, 268-313.

20 C. Ringot, V. Sol, M. Barriere, N. Saad, P. Bressollier, R. Granet, P. Couleaud, C. Frochot and P. Krausz, *Biomacromolecules,* 2011, **12**, 1716-1723.

21 P. Saint-Cricq, T. Pigot, L. Nicole, C. Sanchez and S. Lacombe, *Chem. Commun.,* 2009, **35**, 5281-5283.

22 M. Krouit, R. Granet and P. Krausz, *Eur. Polym. J.,* 2009, **45**, 1250-1259.

23 I. Banerjee, R. C. Pangule and R. S. Kane, *Adv. Mater.,* 2011, **23**, 690-718.

24 O. Lyutakov, Y. Kalachyova, A. Solovyev, J. Svanda, J. Siegel, P. Ulbrich and V. Svorcik, *J. Nanopart. Res.,* submitted.

25 O. Lyutakov, I. Goncharova, K. Kolarova, J. Svanda and V. Svorcik, *Mater. Sci. Eng. C,* submitted.

26 M. Wainwright, M. N. Byrne and M. A. Gattrell, *J. Photochem. Photobiol. B Biol.,* 2006, **84**, 227-230.

27 J. Siegel, K. Kolářová, V. Vosmanská, S. Rimpelová, J. Leitner and V. Švorčík, *Mater. Lett.,* 2013, **113**, 59-63.

28 V. Vosmanská, K. Kolářová, S. Rimpelová, V.Švorčík, *Cellulose,* 2014, **21**, 2445-2456.

29 I. Washio, Y. Xiong, Y. Yin and Y. Xia, *Adv. Mater.,* 2006, **18**, 1745-1749.

30 Z. Shervani, Y. Ikushima, M. Sato, H. Kawanami, Y. Hakuta, T. Yokoyama, T. Nagase, H. Kuneida and K. Aramaki, *Colloid Polym. Sci.,* 2008, **286**, 403-410.

31 T. T. Renjis, A. K. Samal, T. S. Sreeprasad, and T. Pradeep, *Langmuir,* 2007, **23**, 1320-1325.

32 B. Xing, T. Jiang, W. Bi, Y. Yang, L. Li, M. Ma, C. K. Chang, B. Xu, and E. K. L. Yeow, *Chem. Commun.,* 2011, **47**, 1601-1603.

Table 1

Antimicrobial properties (to (i) *P.aeruginosa* and (ii) *S.aureus*) of different coatings "in solution" after different times of treatment without/with illumination. Antimicrobial impact is designated as follow: (-) none; (+/-) weak; (+) apparent.

(i) ***P.aeruginosa***

	Under illumination			**Without illumination**		
Time [min]	30	60	90	30	60	90
$AgNO_3$	+	+	+	+	+	+
AgNPs	+/-	+/-	+	+	+	+
TPP	-	-	+/-	-	-	-
AgNPs + TPP	+/-	+	+	-	-	+/-

(ii) ***S.aureus***

	Under illumination			**Without illumination**		
Time [min]	30	60	90	30	60	90
$AgNO_3$	+/-	+/-	+/-	+/-	+/-	+/-
AgNPs	-	-	-	-	-	+/-
TPP	-	+/-	+	-	-	-
AgNPs + TPP	+	+	+	-	-	+/-

Figure caption

Fig. 1

TEM image of TPP-AgNPs in PMMA films. Blue arrows depict triangular and polygonal Ag nanoparticles.

Fig. 2

Absorption (left) and luminiscence (right) spectra of TPP and TPP-AgNPs in PMMA matrix.

Fig. 3

Silver release from TPP-AgNPs/PMMA films. Part A depicts time dependence of silver concentrations in extracted solution released under light illumination and in dark (study by AAS method). Part B shows depth profile (study by XPS method) of silver concentration in pristine, illuminated and non-illuminated TPP-AgNPs/PMMA films (72 h).

Fig. 4

Absorption spectra of TPP/PMMA, AgNPs/PMMA, and TPP-AgNPs/PMMA treated by water soaking, light illumination, and their combination for different time (for details see the text).

Fig. 5

Absortion spectra of I_2 solution created under illumination of PMMA, TPP/PMMA, and TPP-AgNPs/PMMA films in KI solution. Illumination leads to appearance of reactive oxygen, which initiates I^- to I^0 reductions. Were irradiated fresh samples and samples pretreated during 72 h by light illumination.

Fig. 6

Photos illustrating inhibitory effect on *P.aeruginosa* and *S.aureus* in the presence of illuminated/non-illuminated TPP/PMMA, AgNPs/PMMA, and TPP-AgNPs/PMMA films. The (A) minus signs indicate bacteria growth and absence of antimicrobial effect, the plus/minus signs indicate 50 % growth (B) and plus signs indicate inhibition effect (C).

Fig. 7

Antimicrobial activity against (i) P.aeruginosa and (ii) S.aureus. Ag/TPP-PMMA films were in contact with bacteria on agar for 1 (A), 2 (B), and 3 (C) hours under illumination. Control sample was placed in contact with bacteria but not activated by external light (D). Parts E exhibit light-activated antimicrobial activity of the samples aged for 3 months under environmental conditions.

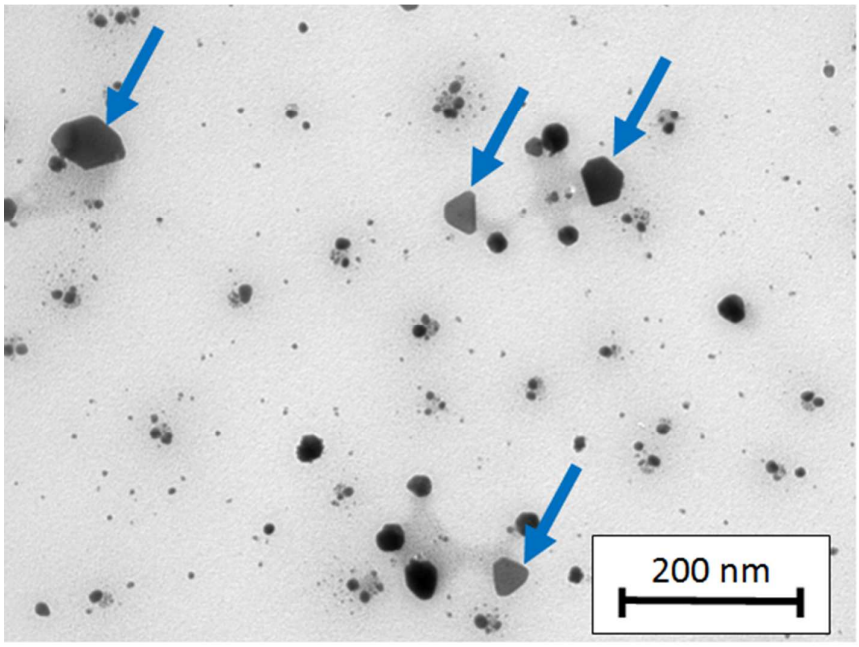

Fig. 1

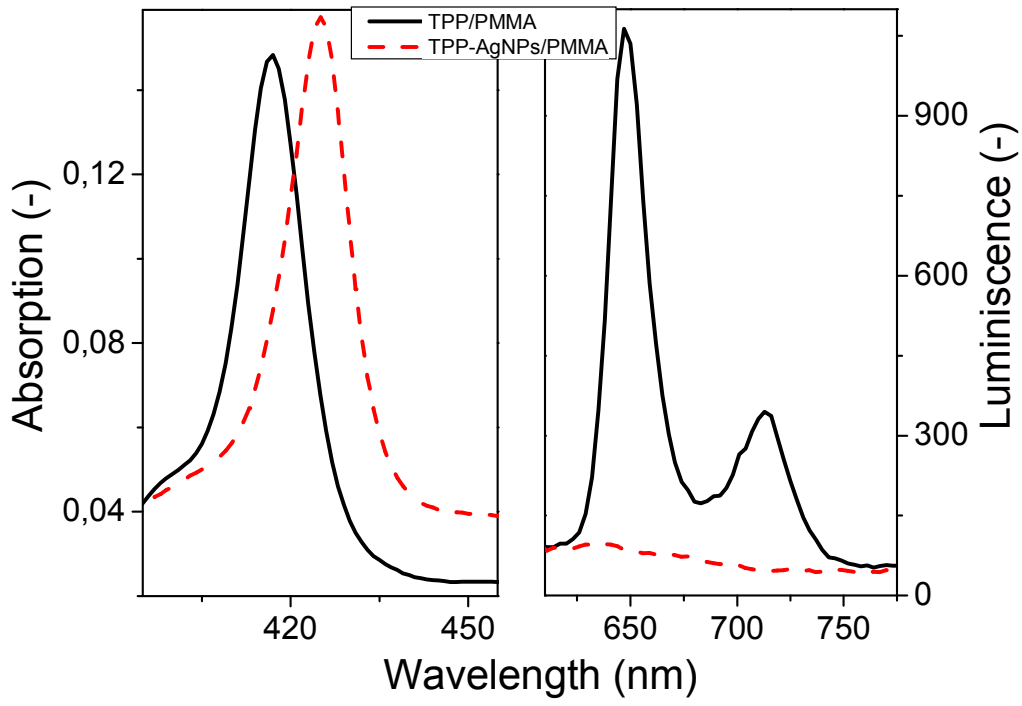

Fig. 2

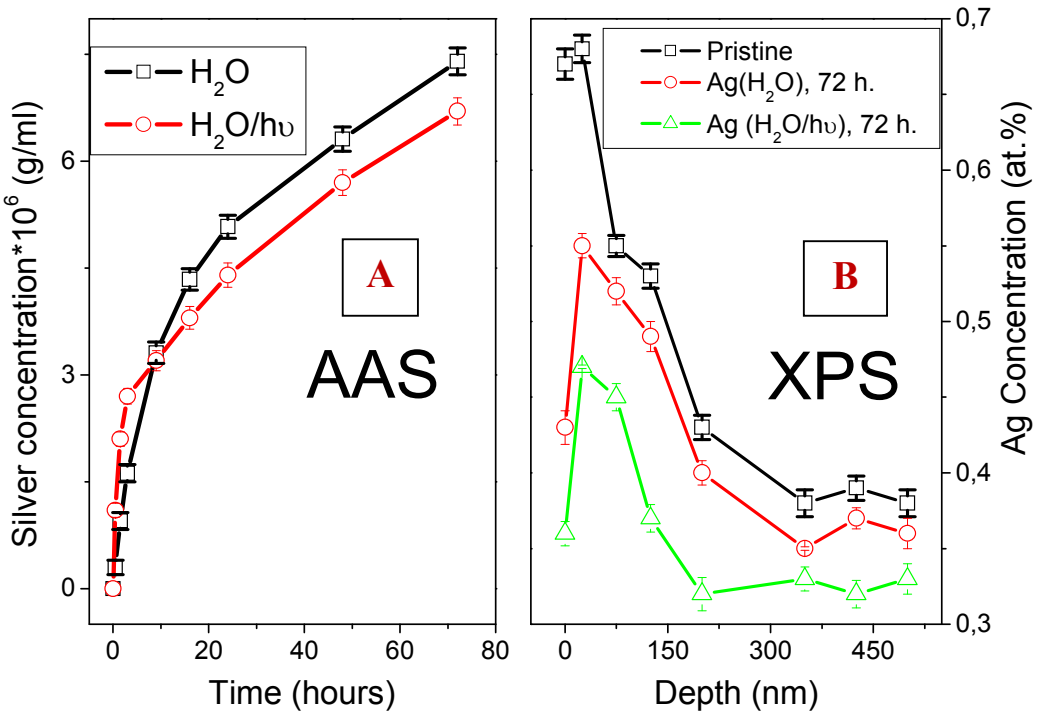

Fig. 3

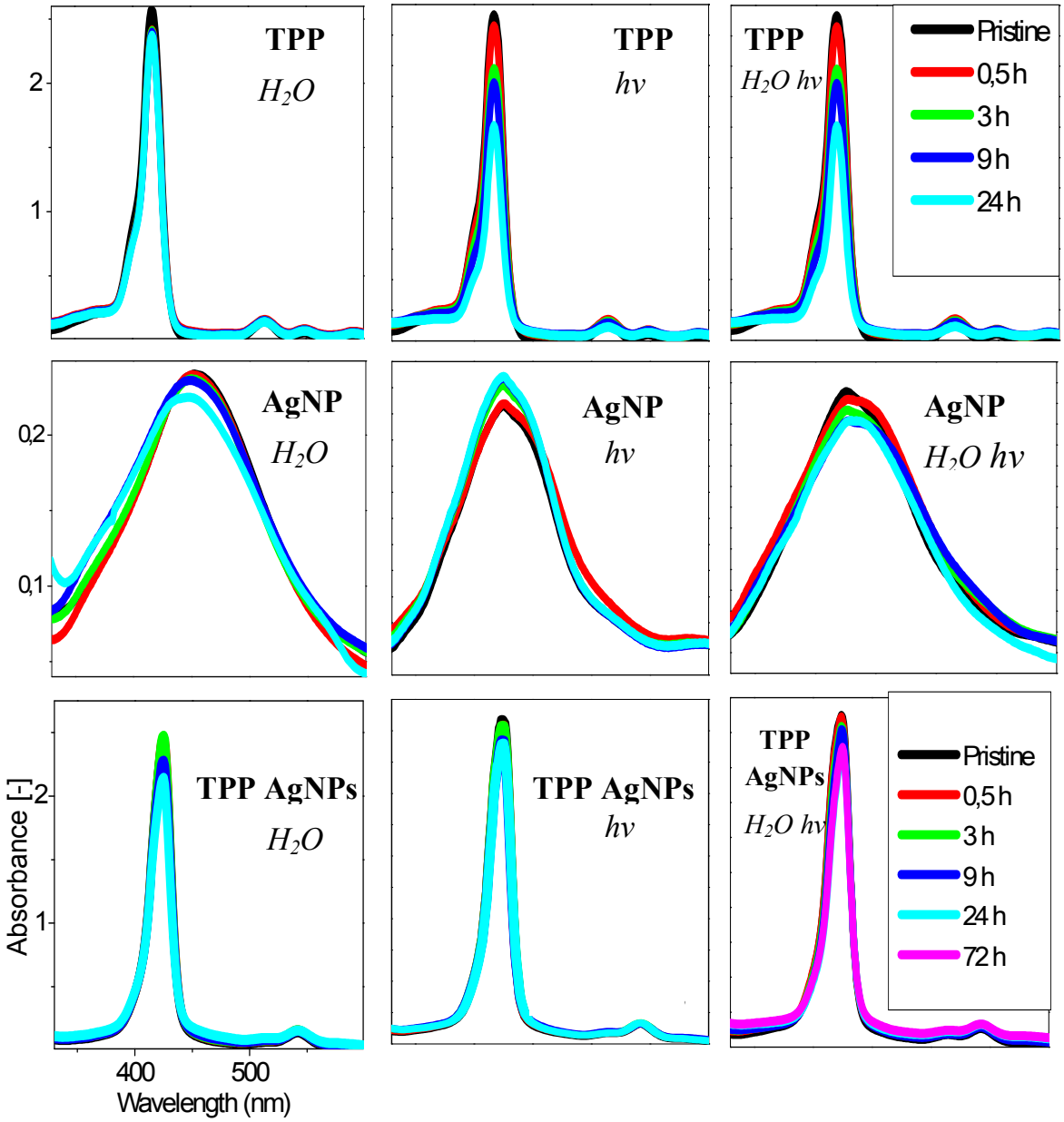

Fig. 4

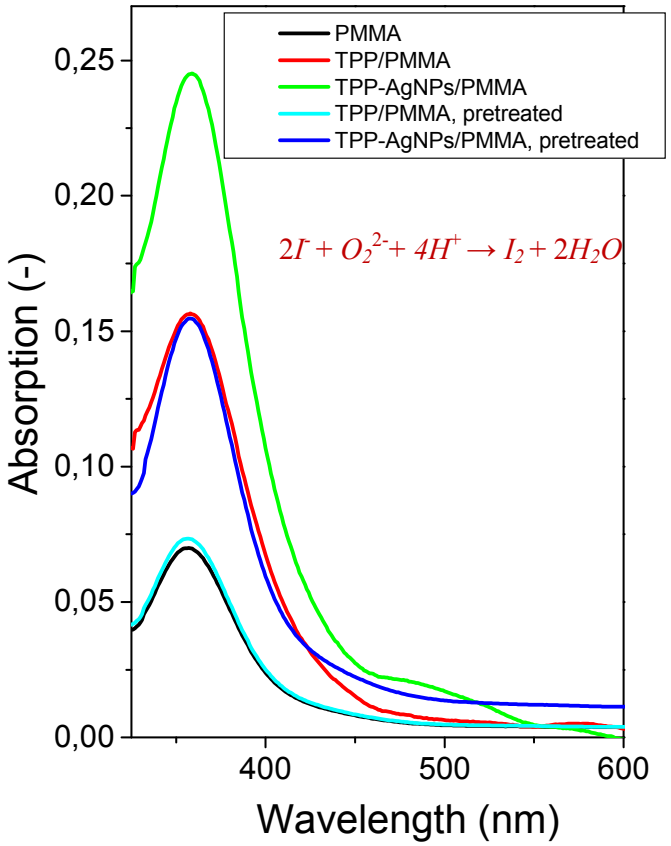

Fig. 5

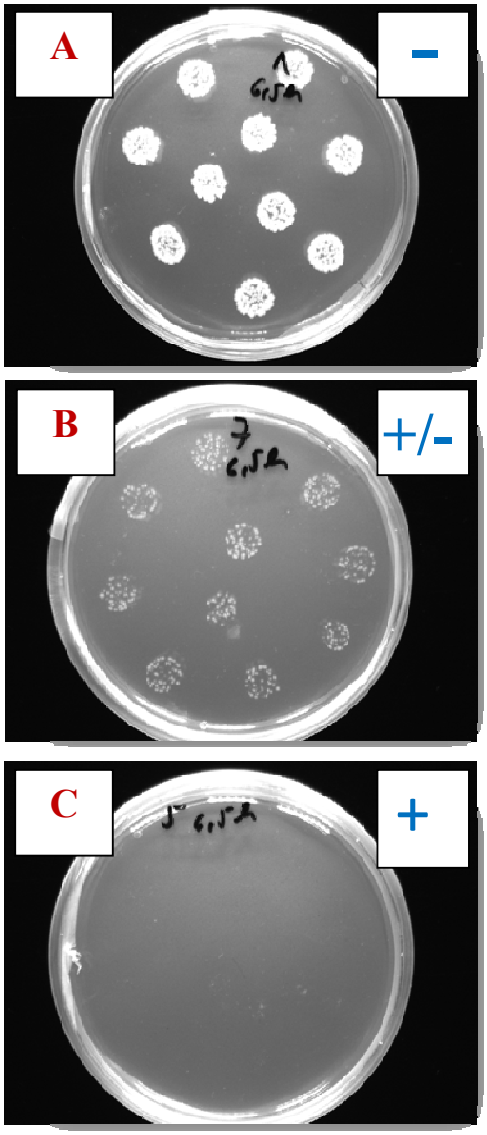

Fig. 6

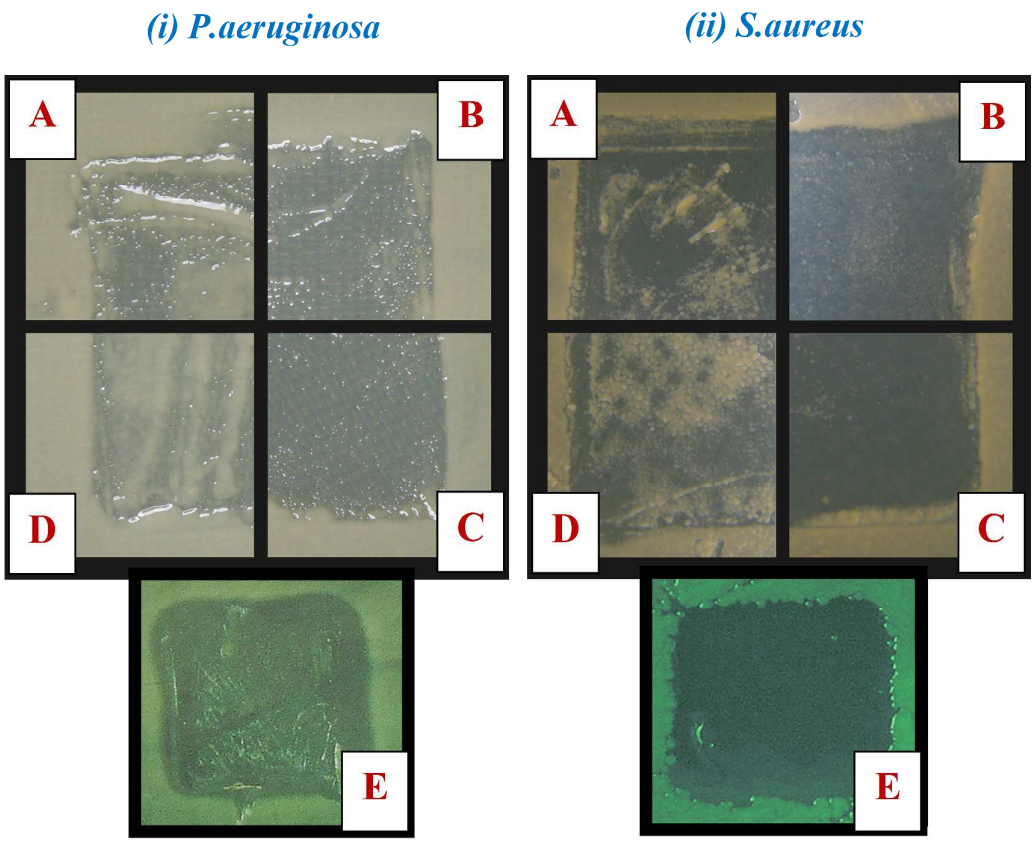

Fig. 7